PFC/JA-95-46

Multiple Plasma Diagnosis from a Five Chord High Energy Resolution X-ray Spectrometer Array

J.E. Rice, F. Bombarda[1], M.A. Graf[2],
E.S. Marmar, J.L. Terry, Y. Wang

November, 1995

[1]Associazone ENEA-Euratom per la Fusione, C.P. 65, 00044 Frascati, Italy.
[2]SRL, Somerville, MA 02143-4241

Submitted to Fusion Engineering and Design.

This work was supported by the U. S. Department of Energy Contract No. DE-AC02-78ET51013. Reproduction, translation, publication, use and disposal, in whole or in part by or for the United States government is permitted.

Multiple Plasma Diagnosis from a Five Chord High Energy Resolution X-ray Spectrometer Array

J. E. Rice, F. Bombarda[+], M. A. Graf[*], E. S. Marmar, J. L. Terry and Y. Wang

Plasma Fusion Center, MIT, Cambridge, MA 02139-4213

[+] *Associazione ENEA-Euratom per la Fusione, C.P. 65, 00044 Frascati, Italy*

[*] *SRL, Somerville, MA 02143-4241*

Abstract

X-ray spectra from Alcator C-Mod plasmas have been collected using a high wavelength resolution five spectrometer array during a wide range of operating conditions, providing a large variety of diagnostic information. Each independently scannable von Hamos type spectrometer has a wavelength range of 2.6 to 4.1 Å, and the complete Rydberg series of He- and Hy-like argon have been observed. Spectra of Δ n = 1 ground state transitions and satellites taken along different chords have been simulated using the results from a collisional-radiative model and the MIST transport code. Line ratios are used to infer the electron temperature profile and good agreement is found with ECE profiles. Line intensities have been used to obtain absolute argon densities and argon recycling coefficients, and up-down asymmetric density profiles are sometimes observed. The widths of the strongest lines have been used to deduce ion temperature profiles, and wavelength shifts have been used to determine toroidal rotation velocities. Transitions from around n = 9 to the ground state are populated by charge-exchange in the outer regions of the plasma and these line intensities have been used to measure neutral hydrogen density profiles. Spectra from helium-like scandium have been obtained during injection experiments and time histories and line intensities have been used to determine impurity transport coefficients. Δ n $\geq$ 2 ground state transitions in molybdenum charge states around neon-like have been observed and used to measure the absolute molybdenum density, and to test atomic structure calculations.

Introduction

In future reactor grade devices, diagnostic access will be severely limited, so efficient use of the space around the machines will be necessary. Care must then be taken in the selection of the essential diagnostics to be used. X-ray emission from high temperature plasmas provides a wealth of information, from the parameter dependences of line intensities and from line shapes. In particular, line widths can be used to measure the ion temperature, line shifts to obtain rotation velocities, line ratios to determine the electron temperature and line intensities to measure the neutral hydrogen density, impurity densities and impurity transport coefficients. The x-ray spectrometer array described here provides these multiple diagnostic capabilities. To take advantage of all of these diagnostic possibilities, it is most convenient to use x-ray emission from helium- and hydrogenlike charge states which exist in the core of the plasma. The elements appropriate for the electron temperature range of the device may come from intrinsic or injected impurities in levels which do not compromise plasma performance.

Experiment Description

Alcator C-Mod[1] is a compact, high magnetic field tokamak with all molybdenum plasma facing components, and the capability of 4MW of ICRF heating[2]. The parameter ranges achieved for the device to date are 2.5 T $\leq B_T \leq$ 6.5 T, .3 MA $\leq I_P \leq$ 1.2 MA, .2 x $10^{14}/cm^3 \leq n_e \leq$ 2.5 x $10^{14}/cm^3$, 1.0 $\leq \kappa \leq$ 1.8 and .7 keV $\leq T_{e0} \sim T_{i0} \leq$ 4.5 keV. Among the many diagnostics is a five chord, high energy resolution x-ray spectrometer array[3,4]. Each spectrometer has a resolving power of 4000, a 2 cm spatial resolution and a luminosity function of 7 x 10^{-13} m^2sr. Each spectrometer can be scanned vertically (with coverage out to the last closed flux surface), and scanned in wavelength between 2.6 and 4.1 Å, with 120 mÅ spanned at a time. This allows for observation of the complete rydberg series in hydrogen- and heliumlike argon. Argon is routinely puffed into C-Mod plasmas through an absolutely calibrated piezoelectric valve, at levels which do not compromise plasma

performance. Metallic impurities can also be injected with a laser blow-off system[5], for impurity transport and atomic physics studies.

Plasma Diagnosis

One of the *raisons d'être* of this diagnostic is to measure the ion temperature and profile under a wide variety of plasma conditions, from the doppler broadening of impurity x-ray lines. The resonance transition, w ($1s^2\ ^1S_0$ - $1s2p\ ^1P_1$) in Ar^{16+} at 3.9492 Å is usually used since it is adequately intense over a range of electron temperatures from 400 to 2500 eV, and due to the relatively low atomic mass (40 AMU), has a large doppler width. For higher temperatures, $Ly_{\alpha 1}$ ($1s\ ^1S_{\frac{1}{2}}$ - $2p\ ^2P_{\frac{3}{2}}$) in Ar^{17+} at 3.7311 Å is appropriate. In the edge regions of the plasma below 400 eV, the forbidden line, z ($1s^2\ ^1S_0$ - $1s2s\ ^3S_1$) in Ar^{16+} is used since it is most intense from population by radiative recombination[6]. An example of the time history of the central ion temperature from x-ray doppler measurments is shown in Fig.1, and compares favorably with the results from the neutron counter[7]. This particular discharge had ICRF and lithium pellet injection. During the PEP mode[8] at .83 sec, the ion temperature profile became very peaked, going from a HWHM of 9.2 cm at .7 sec, to 6.7 cm at .83 sec. While the time resolution of the x-ray temperature is not as good as from the neutrons, the x-ray measurement does not depend upon an absolute intensity calibration, *a priori* knowledge of the ion temperature profile and deuteron density, and yields ion temperatures in hydrogen plasmas. The major source of uncertainty in the x-ray measurement is the contribution of the instrumental width to the overall doppler width of the line of interest.

From the position (wavelength) of the x-ray lines, the impurity rotation velocity may be determined. For this measurement the Ar^{17+} $Ly_{\alpha 1}$ is used, which has the advantage that there is a nearby potassium line[9] which can be used for a wavelength calibration. The maximum toroidal rotation velocities measured so far in ohmic discharges are $\sim$ 6 x 10^6 cm/sec, in the same direction as the *electrons*, at the beginning of the discharge, when the loop voltage is highest.

Another diagnostic application of this x-ray spectrometer system is the measurement of the electron temperature from line ratios. Advantage can be taken of the different temperature dependences of individual line population mechanisms, or in the temperature dependence of ionization state balance[10]. The brightness ratio of the 1s $^1S_{\frac{1}{2}}$ - 3p $^2P_{\frac{3}{2}}$ transition in Ar^{17+} (3150.24 mÅ) to the $1s^2$ $^1S_0$ - 1s5p $^1P_1$ transition in Ar^{16+} (3128.47 mÅ) is sensitive to the electron temperature[11] in the range from 1 to 2.5 keV, mainly due to differences in the ionization rates. Shown in Fig.2 by the solid curve is the calculated brightness ratio of these two lines as a function of electron temperature (actually *vice versa*), where coronal equilibrium[12] is assumed, and a typical electron temperature profile shape[13] is used. The assumption of coronal equilibrium is well taken in the plasma center[6]. Shown in Fig.2 by the asterisks are the measured central chord brightness ratios as a function of electron temperature measured by the electron cyclotron grating polychromator[14], and the agreement is very good. It's also possible to determine the electron temperature from line ratios originating from the same ionization state, from lines populated by collisional excitation and dielectronic recombination[15,4] (w and the satellite k), which has the advantage of eliminating the coronal equilibrium assumption.

High n transitions in Ar^{16+} can be used to determine the neutral hydrogen density in the plasma[16]. The $1s^2$ $^1S_0$ - 1s9p $^1P_1$ and $1s^2$ $^1S_0$ - 1s10p $^1P_1$ transitions have large rate coefficients for population by charge exchange recombination[17]. Shown in Fig.3 are spectra taken in the vicinity of these lines. The solid line shows the spectrum from a line of sight through the bottom of the machine (r/a = .7), and the enhancement of the n=9 and n=10 is apparent. The very high n lines around n=20 are also visible, from charge exchange with excited neutral hydrogen[16]. The spectrum shown by the dotted lines is from the same flux surface (r/a = .7), but from the top of the machine, and there is no evidence for enhancement from charge exchange recombination. This indicates that the neutral hydrogen density is nearly a factor of 10 higher in the bottom of the machine than in the top. For this particular discharge, the X-point was located in the bottom, and in these discharges, there is an enhancement of the Hα emission[18] and C^{2+} emission[19] in the bottom of

the machine.

From the absolute line brightnesses, impurity densities and profiles may be determined[20,21]. Since the piezoelectric valve used to inject the argon is absolutely calibrated, impurity screening or penetration efficiencies may be determined. The penetration efficiency is defined here to be the ratio of the the number of atoms in the plasma core to the number of atoms injected. The penetration of argon is shown in Fig.4 as a function of electron density for limited and diverted plasmas. For both configurations, the penetration is reduced at higher electron densities[22,5,20], which is consistent with observations of intrinsic impurity levels. The penetration is also reduced when going to diverted operation, demonstrating one advantage over the limiter configuration. In any case, the penetration of impurities into Alcator C-Mod is small, in most instances less than 3%.

In addition to the previously mentioned diagnostic capabilities, the x-ray spectrometer system can also provide information relating to plasma and atomic physics studies. In particular, asymmetries in up-down line brightness profiles can provide information on impurity drifts, while studies of x-ray spectra from neonlike molybdenum[23] have been used to benchmark atomic structure calculations.

Conclusions

The multiple diagnostic capabilities of the x-ray spectrometer array on Alcator C-Mod have been demonstrated. This one diagnostic system is able to provide $T_i(r,t)$, $T_e(r,t)$, $V_{Tor}(t)$, $n_0(r)$, $n_I(r,t)$, in addition to impurity transport coefficients and information pertaining to atomic and plasma physics studies.

Acknowledgements

The authors would like to thank J. Irby for electron density measurements, A. Hubbard for electron temperature measurements and the Alcator C-Mod operations group for expert running of the tokamak. Work supported at MIT by DoE Contract No. DE-AC02-78ET51013.

References

[1] I.H.Hutchinson et al., Phys. Plasmas **1**, 1511 (1994)

[2] S.N.Golovato, M. Porkolab, Y. Takase et al., in *Proceedings of the 11th Topical Conference on Radio-Frequency Power in Plasmas*, Palm Springs, CA (AIP, New York, 1995), (to be published).

[3] J.E.Rice and E.S.Marmar, Rev. Sci. Instrum. **61**, 2753 (1990)

[4] J.E.Rice et al., Rev. Sci. Instrum. **66**, 752 (1995)

[5] M.A.Graf et al., Rev. Sci. Instrum. **66**, 636 (1995)

[6] J.E.Rice et al., Phys. Rev. A **35**, 3033 (1987)

[7] C.L.Fiore and R.L.Boivin, Rev. Sci. Instrum. **66**, 945 (1995)

[8] Y.Takase et al., Controlled Fusion and Plasma Physics (Proc. 22nd European Physical Society Conference, Bournemouth, UK, 3-7 July 1995) Vol. 19C, p. II-341 (1995)

[9] E.S.Marmar et al., Phys. Rev. A **33**, 774 (1986)

[10] G.Bekefi, C.Deutsch and B.Yaakobi, in "Principles of Laser Plasmas", edited by G.Bekefi (Wiley, New York, 1976), pp.593-596

[11] J.E.Rice et al., Rev. Sci. Instrum. **57**, 2154 (1986)

[12] C.Breton et al., Association Euratom-C.E.A., Fontenay-aux-Roses, France, Report No. EUR-CEA-FC-948 (1978)

[13] T.C.Hsu et al., Proc. 8th Joint Workshop on ECE and ECRH, IPP III/186, 409 (1993)

[14] P.J.Oshea et al., Proc. 9th Joint Workshop on ECE and ECRH (EC-9), Borrego Springs, CA, (1995)

[15] J. Dubau and S. Volonte, Rep. on Prog. in Physics, **43**, 199 (1980)

[16] J.E.Rice et al., Phys. Rev. Lett. **56**, 50 (1986)

[17] R.K.Janev et al., Phys. Rev. A **28**, 1293 (1983)

[18] C.Kurz et al., Rev. Sci. Instrum. **66**, 619 (1995)

[19] J.L.Terry et al., Rev. Sci. Instrum. **66**, 555 (1995)

[20] J.E.Rice et al., J. Phys. B **28**, 893 (1995)

[21] J.E.Rice et al., submitted to J. Phys. B

[22] G.M.McCracken et al., J. Nucl. Mater. **220**, 264 (1995)

[23] J.E.Rice et al., Phys Rev A **51**, 3551 (1995)

Figure Captions

Fig. 1 Time histories of the ion temperature from x-rays (asterisks) and neutrons (solid curve). There was a lithium pellet injection at .76 s (vertical line) and ICRF from .775 to 1.1 s, which peaked at 2.5 MW.

Fig. 2 The electron temperature versus calculated brightness ratio (Ar^{17+} 1s-3p to Ar^{16+} $1s^2$-1s5p) is shown by the solid curve, and the measured electron temperatures versus measured line ratios are shown by asterisks.

Fig. 3 High n x-ray spectra from the bottom (solid curve) and top (dotted lines) of the machine for a lower point X-point discharge.

Fig. 4 Argon penetration (argon atoms in the plasma core/argon atoms injected) as a function of electron density for limited (dots) and diverted (asterisks) discharges.

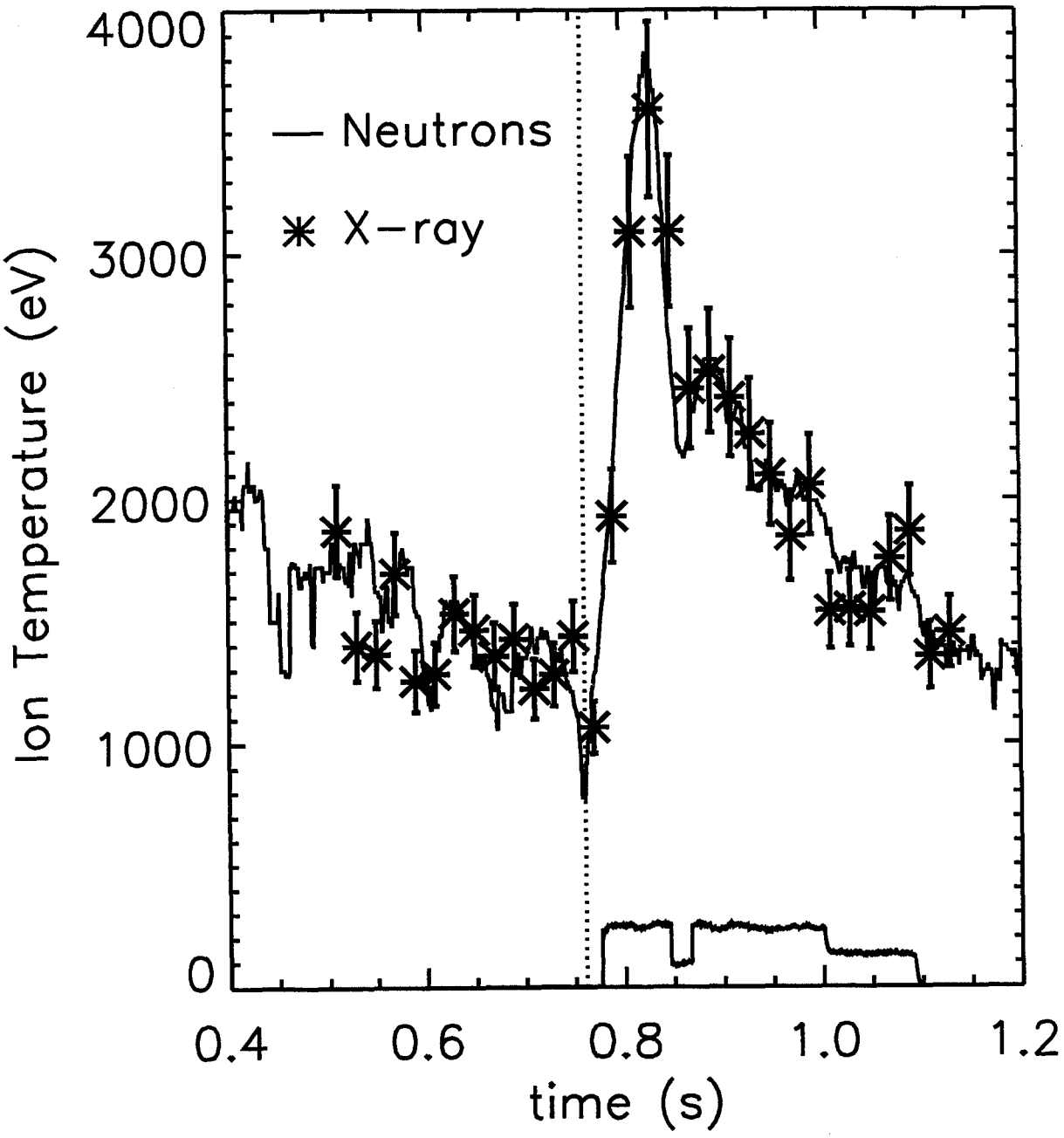
4000
3000
2000
1000
0
Ion Temperature (eV)
— Neutrons
* X-ray
0.4
0.6
0.8
1.0
1.2
time (s)

Figure 1

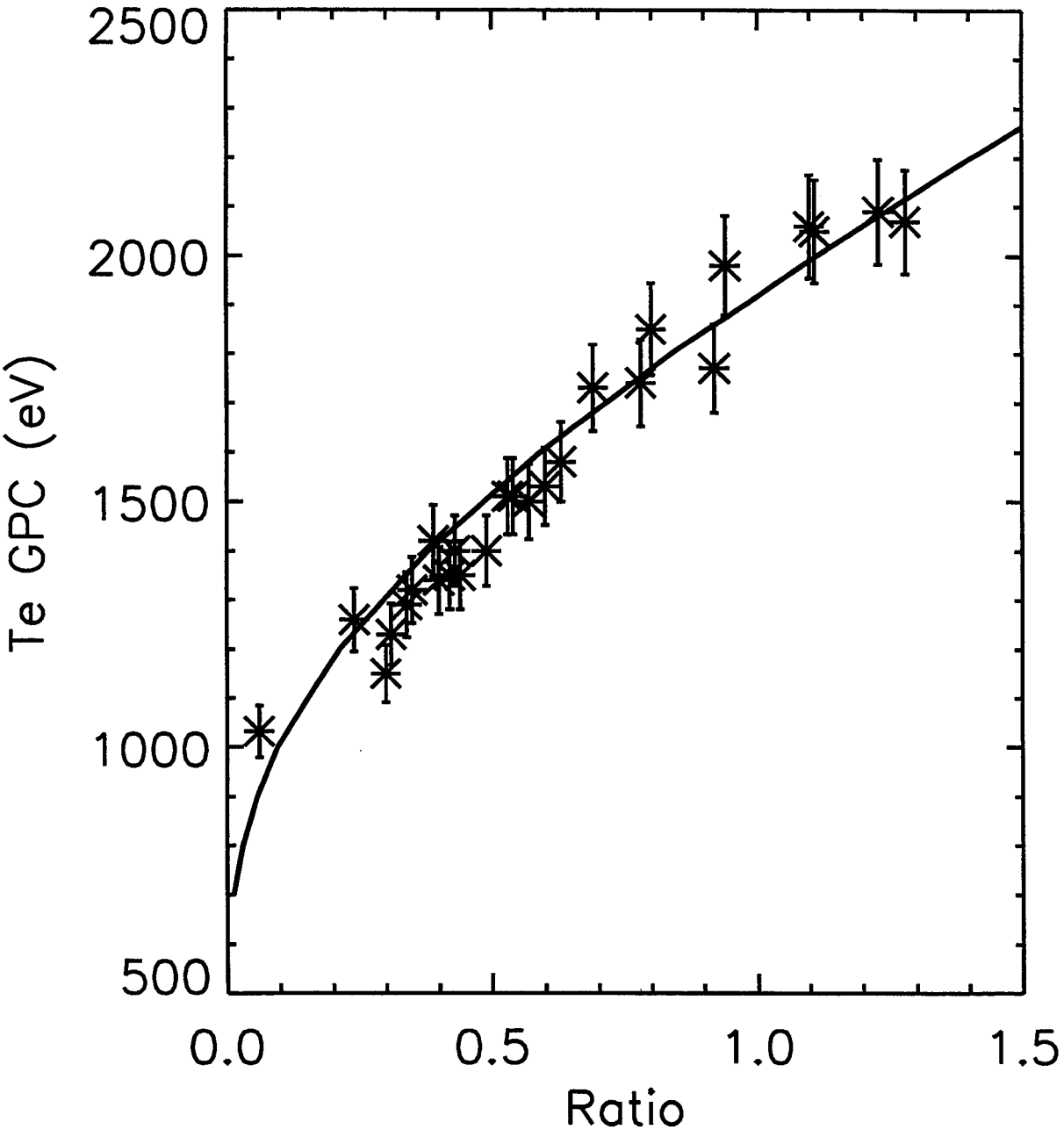

Figure 2

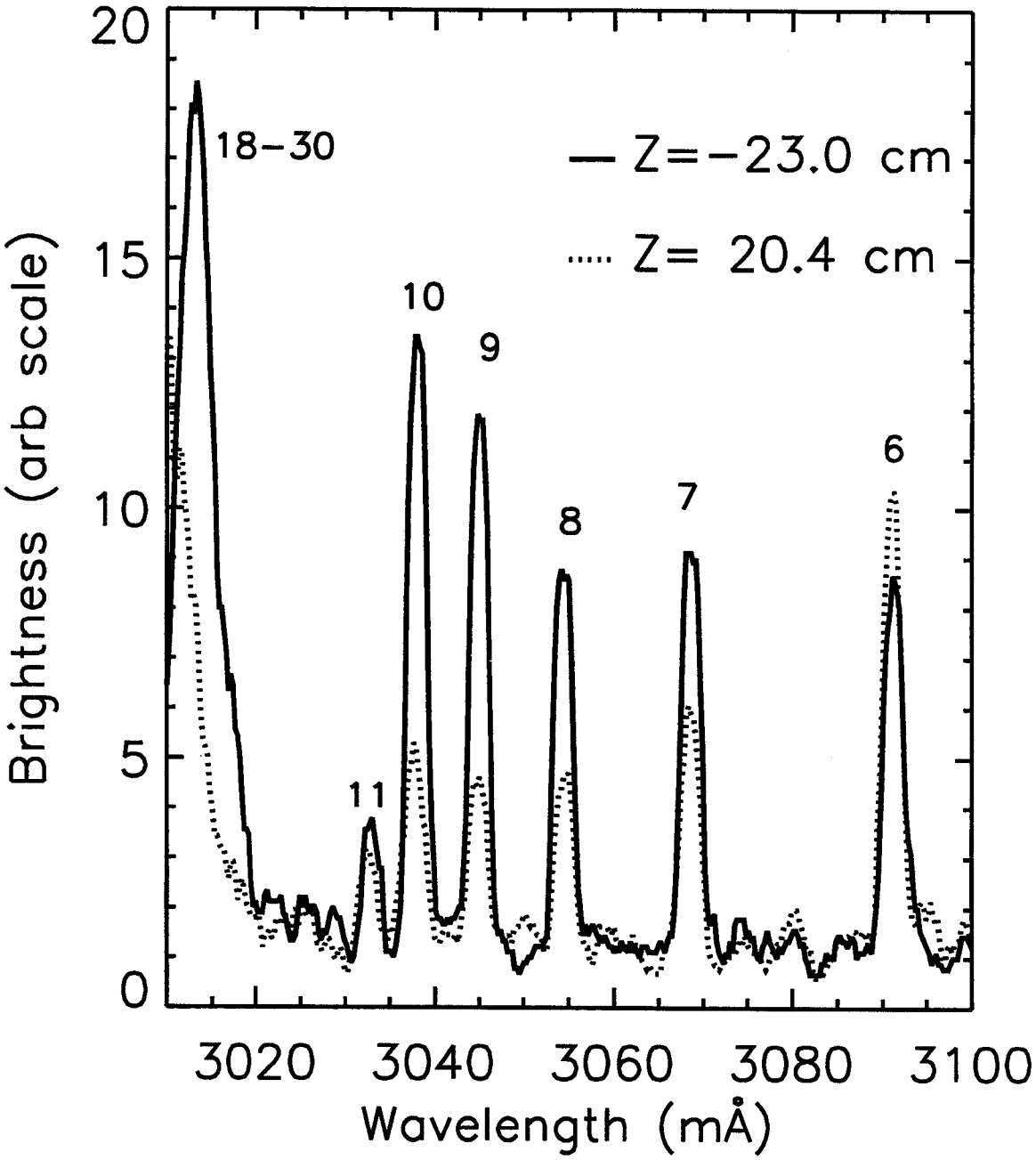
20
15
10
5
0
Brightness (arb scale)
18-30
— Z=-23.0 cm
····· Z= 20.4 cm
11
10
9
8
7
6
3020
3040
3060
3080
3100
Wavelength (mÅ)

Figure 3

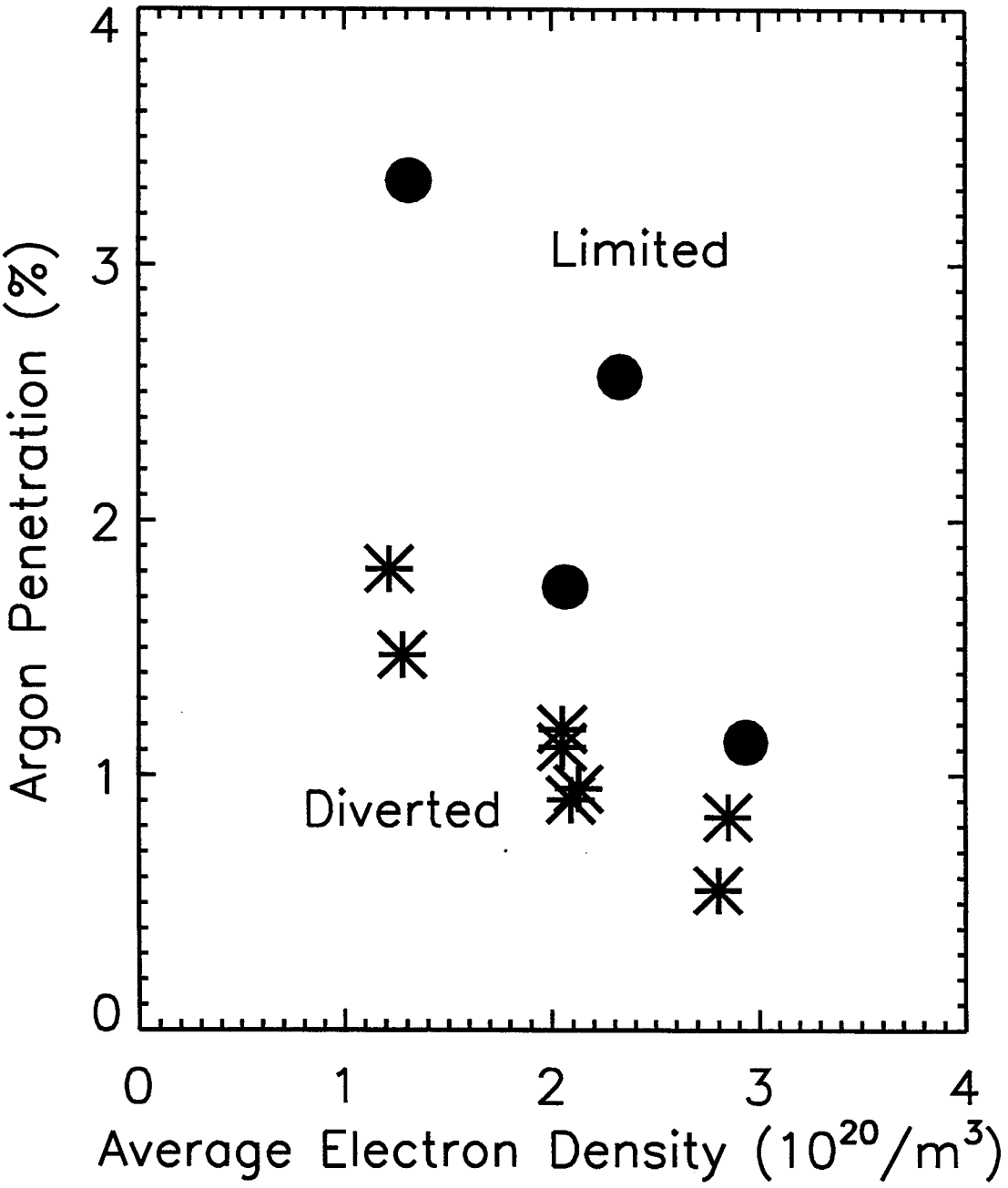
Argon Penetration (%)
Average Electron Density ($10^{20}/m^3$)
Limited
Diverted
0
1
2
3
4

Figure 4